JTTEE5 6:305-308

On Cavities in Thermally Spheroidized Powder Particles*

R. Klíma and P. Kotalík

A melted spherical particle begins to solidify on cooling, and the radius of the first thin solid layer is approximately equal to the radius of the melted particle. Since the density of the solid phase is higher than that of the liquid one, porosity forms inside the sphere during further solidification. The pressure in the remaining melted material may decrease considerably. The requirement for a pressure balance implies that a relationship for the pore radius can be derived. The pore arises as a bubble in a boiling liquid. The bubble stability and its minimum radius are derived, as well as conditions for its formation. It is shown that, at most, one bubble can occur in the particle.

Analytical results are applied to the case of alumina particles, and the growing process of the cavity is simulated. Craters found on some spheroidized particles stem from asymmetry of the solid shell formation and the simultaneous action of the atmospheric pressure. The practical importance of this effect is that additional porosity may be formed in thermal spray products.

Keywords alumina powder, bubble formation in liquids, closed porosity, solidification of melted particles, thermally spheroidized powder

1. Introduction

Hollow spheres are often obtained during spheroidization of fine powder grains with the aid of, for example, plasma jets (Ref 1, 2). Small cavities arise due to the higher density of the solidifying surface layer compared to the melted phase and when very fast cooling does not allow compression under atmospheric pressure (Ref 1).

The presence of cavities inside particles (see Fig. 1) leads to a lower density of the powder and, consequently, to additional porosity of the final products. Therefore, a more detailed analysis of that phenomenon may be desirable.

The purpose of this paper is to give a simple physical theory of cavity formation. Our study is based mostly on standard thermodynamics, with inhomogeneities connected with the crystal structures being neglected. Although this approach is not completely rigorous, it is used as a first approximation.

In what follows, the conditions to form cavities in quickly cooled solidifying particles are derived, possible motions of the cavities are pointed out, and the final volume of a cavity is calculated. The results are supported by a computer simulation of particle cooling and cavity growth.

2. Physical Model

2.1 *Pressure Evolution in the Melted Phase*

Assume a completely melted spherical particle with only radial dependence of temperature. If cooling of the particle is spherically symmetric, a solid layer grows at the entire particle surface. Since the mass density of the solid phase, ρ_s, is higher than the density of the melted one, ρ_m, the hydrostatic pressure in the melted phase decreases. Simultaneously, the sphere radius, R_0, can decrease due to the atmospheric pressure. We assume that cooling is sufficiently fast that this sphere deformation is negligible. Thus, the radius R_0 of the first thin solid shell is constant.

Consider the pressure variations in the melted phase before formation of the cavity. Let R_m be the radius of the melted material, the layer between R_m and R_0 being solid. If the solidification steps by $|\Delta R_m|$ toward the sphere center, the remaining melted material is subjected to a volume dilatation of:

$$\Delta V_p = \left(1 - \frac{\rho_m}{\rho_s}\right) 4\pi R_m^2 |\Delta R_m| > 0 \qquad \text{(Eq 1)}$$

given by the increase of the mass density from ρ_m to ρ_s during the phase transition. The corresponding decrease of the pressure in the melted region is:

$$\Delta P = -\frac{\Delta V_p}{\kappa V} \qquad \text{(Eq 2)}$$

where κ is the coefficient of the volume compressibility and V is the volume of the melted phase. Using Eq 1 in Eq 2 and limiting $\Delta R_m \to 0$, we obtain:

$$\frac{dP}{dR_m} = \frac{3}{\kappa R_m}\left(1 - \frac{\rho_m}{\rho_s}\right) \qquad \text{(Eq 3)}$$

a relation giving the dependence of the pressure in the whole melted region on its radius R_m:

$$P(R_m) = P_1 - \frac{3}{\kappa}\left(1 - \frac{\rho_m}{\rho_s}\right) \ln \frac{R_0}{R_m} \qquad \text{(Eq 4)}$$

R. Klíma and **P. Kotalík,** Institute of Plasma Physics, Academy of Sciences of Czech Republic, Za Slovankou 3, P.O. Box 17, 182 00 Prague 8, Czech Republic, klima@ipp.cas.cz, kotalik@ipp.cas.cz.

*This work was partially sponsored by GA CR Grant No. 106/93/0638.

where P_1 is the atmospheric pressure (equal to initial pressure in the melted drop). Thermal dilatations different from ΔV_p and possible variations of κ have been neglected.

2.2 *Bubble Formation*

According to the Clausius-Clapeyron equation, the boiling point temperature decreases with pressure decrease. In fact, the pressure of the melted phase can even reach, for a moment, negative values at early stage of the solidification. Therefore, a bubble arises in the region of the highest temperature of the melt. If the radius of the (supposedly spherical) bubble is $R_b << R_m$, the pressure of the melted phase increases by:

$$\Delta P \simeq \frac{R_b^3}{\kappa R_m^3} \qquad \text{(Eq 5)}$$

Due to the surface tension, σ, the pressure inside the bubble is $2\sigma/R_b$ higher.

Symbols

F	Force due to surface tension
M	Molecular mass in atomic units
P_1	Atmospheric pressure
P_v	Tension of vapors in the bubble
ΔP	Decrease of melted phase pressure
q	Heat of evaporation
R	Variable radius
R_0	Radius of the initial droplet
R_b	Bubble radius
R_b^{min}	Minimum bubble radius
R_{b1}	Radius of the unstable bubble
R_{b2}	Radius of the stable bubble
R_c	Radius of the final cavity
R_g	Universal gas constant
R_m	Radius of the melted material
ΔR_{atm}	Particle radius decrease owing to the atmospheric pressure
ΔR_m	Solidification step toward the sphere center
ΔR_s	Thickness of the solid shell ($= R_0 - R_m$)
ΔV_p	Melted material dilatation due to ΔR_m
T	Local temperature in the melted phase
T_1	Boiling point temperature at P_1
T_b	Temperature in the bubble
T_{cr}	Critical temperature
T_m	Melting point temperature
T_{max}	Maximum temperature in the melted material
V	Volume of the melted phase
V_0	Volume of the initial droplet
V_c	Volume of the final cavity
V_{ce}	Experimentally found cavity volume
α_v	Coefficient of thermal volume dilatation
κ	Coefficient of volume compressibility
μ	Viscosity of the melted material
ρ_m	Density of the melted phase
ρ_s	Density of the solid phase
σ	Surface tension

Let us introduce the thickness of the solid shell, $\Delta R_s = R_0 - R_m$. Accounting for only first-order terms $\Delta R_s/R_0$ in Eq 4 and neglecting them in Eq 5, we obtain the equation of pressure equilibrium in the bubble as:

$$P_v - P_1 + \frac{3}{\kappa}\left(1 - \frac{\rho_m}{\rho_s}\right)\frac{\Delta R_s}{R_0} = \frac{R_b^3}{\kappa R_0^3} + \frac{2\sigma}{R_b} \qquad \text{(Eq 6)}$$

where P_v is the tension of vapors in the bubble, $P_v < P_1$. P_v could be found from the data given in Ref 3, or determined approximately from the relation:

$$P_v \simeq P_1 \exp\left[\frac{q}{R_g}\left(\frac{1}{T_1} - \frac{1}{T_b}\right)\right] \qquad \text{(Eq 7)}$$

where q is the heat of evaporation, R_g is the universal gas constant, T_1 is the boiling point temperature at the atmospheric pressure P_1, and T_b is the temperature in the bubble. Considerable discrepancies have been found in the literature concerning the q and P_v values in the case of Al_2O_3. However, useful information can be extracted from Eq 6 without determining the value of P_v. Note that the left-hand side of the equation increases linearly with ΔR_s from a negative value at $\Delta R_s = 0$. The right-hand side of Eq 6 is positive for all values of the bubble radius R_b. The algebra of this expression implies that:

- At a given ΔR_s, two real values, R_{b1} and R_{b2} ($R_{b1} \le R_{b2}$), satisfy Eq 6.
- The right-hand side of Eq 6 as a function of R_b has a single minimum at:

$$R_b^{min} = R_0\left(\frac{2\sigma\kappa}{3R_0}\right)^{1/4} \qquad \text{(Eq 8)}$$

  Note that this value does not depend on ρ_s and ρ_m.
- The minor root $R_{b1} \le R_b^{min}$ is unstable.
- Therefore, the stable solution of Eq 6 is:

$$R_b = R_{b2} > R_b^{min} \qquad \text{(Eq 9)}$$

The minimum value of the right-hand side of Eq 6 (multiplied by κ) corresponding to the value of R_b^{min} is approximately:

$$\frac{7}{4}\left(\frac{2\sigma\kappa}{R_0}\right)^{3/4}$$

Thus, the solution of Eq 6 exists if:

$$\kappa(P_v - P_1) + 3\left(1 - \frac{\rho_m}{\rho_s}\right)\frac{\Delta R_s}{R_0} \ge \frac{7}{4}\left(\frac{2\sigma\kappa}{R_0}\right)^{3/4} \qquad \text{(Eq 10)}$$

In other words, this inequality is the condition of existence of the stable bubble. Since $P_v < P_1$, the *necessary* condition for this is:

$$\frac{\Delta R_s}{R_0} \ge \frac{7}{12}\left(\frac{2\sigma\kappa}{R_0}\right)^{3/4}\left(1 - \frac{\rho_m}{\rho_s}\right)^{-1} \qquad \text{(Eq 11)}$$

On the other hand, the *sufficient* condition for the existence of the bubble is obtained by deleting the unknown value of P_v:

$$\frac{\Delta R_s}{R_0} \geq \frac{1}{3}\left(1-\frac{\rho_m}{\rho_s}\right)^{-1}\left[\frac{7}{4}\left(\frac{2\sigma\kappa}{R_0}\right)^{3/4}+\kappa P_1\right] \quad \text{(Eq 12)}$$

These relations are used in section 3 for practical estimates.

2.3 *Bubble Motion in Temperature Gradient*

Surface tension, σ, decreases with increasing temperature, T (Ref 3):

$$\frac{d\sigma}{dT} = -B\left(\frac{\rho_m}{M}\right)^{2/3} \quad \text{(Eq 13)}$$

where M is the molecular mass in atomic units and $B = 2.1 \times 10^{-5} kg^{1/3} m^2 s^{-2} K^{-1}$. If the temperature in the vicinity of the bubble is inhomogeneous, the pressure $2\sigma/R_b$ is also inhomogeneous. Assuming that, near the bubble, the temperature changes slightly with respect to the bubble diameter, we integrate the pressure $2\sigma/R_b$ over the bubble surface to obtain the net force acting on the bubble:

$$\mathbf{F} \simeq -\frac{8}{3}\pi R_b^2 \frac{d\sigma}{dT}\,\text{grad}\,T \quad \text{(Eq 14)}$$

In other words, the force $-\mathbf{F}$ acts on the liquid adjacent to the bubble. Consequently, the bubble moves with velocity $\mathbf{v}$, given by the balance of the force $\mathbf{F}$ and the viscous drag (Ref 4):

$$\mathbf{v} \simeq -\frac{2R_b}{3\mu}\frac{d\sigma}{dT}\,\text{grad}\,T \quad \text{(Eq 15)}$$

where μ is the viscosity of the melted material. As a result, a bubble born in a region of inhomogeneous temperature will move toward the temperature maximum.

2.4 *Volume of the Final Cavity*

Concluding this section, we present an expression for the volume, V_c, of the resulting cavity in the solidified spherical drop. According to our idealized model of zero deformation by atmospheric pressure, V_c equates to the difference between the volumes of the melted and solid matter. This is calculated by considering the inverse process, namely, melting of the solid particle. In this case, unlike the previous discussion, the thermal dilatation of the melted drop is included. Integration over the volume, V_0, of the spheric drop gives:

$$\frac{V_c}{V_0} \simeq 1 - \frac{\rho_m}{\rho_s} + \frac{3\alpha_v}{R_0^3}\int_0^{R_0}[T(R) - T_m]\,R^2 dR \quad \text{(Eq 16)}$$

where α_v is the coefficient of thermal volume dilatation, T_m is the melting point temperature, and $T(R)$ is the local temperature at the moment of the sphere surface solidification. The last term in Eq 16 is often negligible. Then,

$$\frac{R_c}{R_0} \simeq \left(1-\frac{\rho_m}{\rho_s}\right)^{1/3} \quad \text{(Eq 17)}$$

is a simple estimate of the cavity radius R_c.

3. Estimates for Alumina Particles

The mass densities of melted and solid Al_2O_3 are $\rho_m = 2750$ kg/m^3 and $\rho_s = 3900$ kg/m^3. The value of the surface tension is estimated by using Eq 13, where now $M = 102$:

$$\frac{d\sigma}{dT} \simeq -1.9 \times 10^{-4}\ \text{N/mK} \quad \text{(Eq 18)}$$

This is integrated from the critical temperature, T_{cr}, where $\sigma = 0$, to the maximum temperature, T_{max}, in the melted phase. According to Ref 3, a rough estimate is $T_{cr} \simeq T_l/0.64$, $T_l \doteq 3000$ °C, and, therefore, $T_{cr} \simeq 4700$ °C.

The value of T_{max} is given by numerical modeling that is based on improving the finite-element method used in Ref 5 to model the thermal evolution of alumina particles in a plasma jet. The improvement takes into account the volume changes due to solidification so that precise mass conservation is achieved. Without going into details on the transport coefficients needed (these are summarized in Ref 5), Fig. 2 indicates the temperature profiles for an Al_2O_3 particle of 30 μm radius and an initial temperature of 2800 K. Particle cooling was driven by Newton's law with constant values of an external environment temperature and heat-transfer coefficient, 500 K and 10^5 W/m$^2 \cdot$ K, respectively. We see that T_{max} at the moment of bubble formation is about 2470 K. Then, from Eq 18:

$$\sigma \simeq 1.9 \times 10^{-4}(T_{cr} - T_{max}) \simeq 0.5\ \text{N/m} \quad \text{(Eq 19)}$$

No data have been found concerning the value of compressibility coefficient κ for melted alumina. The values of κ given in the literature (e.g., Ref 3) for very different liquids are, in almost all cases, on the order of 10^{-9} Pa^{-1}. This value is used in the present calculations. Possible error in κ implies almost the same error in quantities $\Delta R_s/R_0$ (given by Eq 11 and 12), which,

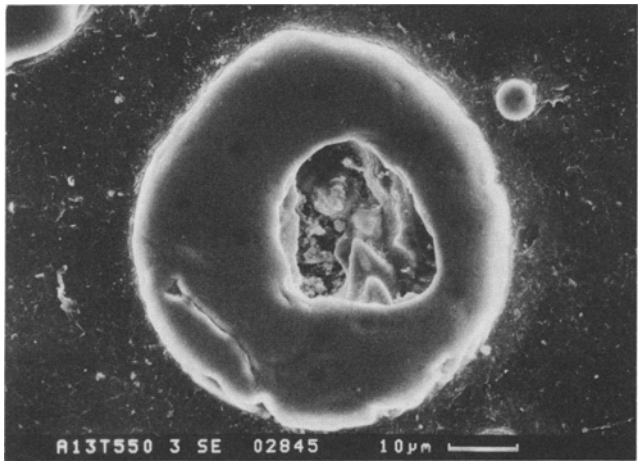

Fig. 1 Cross section of a hollow $Al_2O_3 + 13TiO_2$ particle. Courtesy of B. Kolman

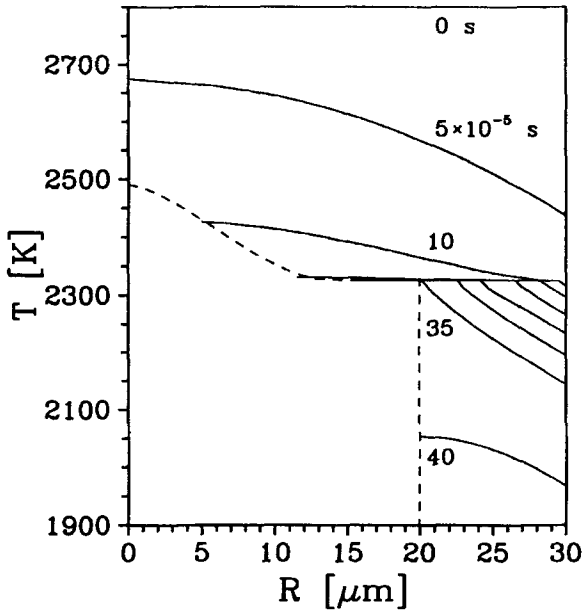

Fig. 2 Temperature profiles in 30 μm Al_2O_3 particle at the times $n \times 5 \times 10^{-5}$ s, $n = 0, 1, \ldots, 8$ (solid lines) and cavity surface temperature during solidification (dashed line)

however, remain very small. The value of R_b^{min} in Eq 8 is much less sensitive to variations in κ due to the exponent ¼.

Let us consider a solidifying alumina droplet with the above-mentioned values of ρ_m, ρ_s, T_{max}, σ, κ, and radius $R_0 = 30$ μm. The necessary condition (Eq 11) to give rise to a stable bubble is $\Delta R_s/R_0 \geq 8 \times 10^{-4}$. The sufficient condition (Eq 12) is $\Delta R_s/R_0 \geq 9 \times 10^{-4}$. These two values of the solid shell thickness are almost equal and very small. Consequently, the bubble arises immediately after the start of solidification.

The minimum bubble radius is given by Eq 8 and 9, $R_b^{min}/R_0 \simeq 1/20$. We remark that the pressure of surface tension $2\sigma/R_b^{min}$ is about 0.6 MPa, a considerable value.

The velocity driven by the temperature gradient here is:

$$v \simeq 1.3 \times 10^{-4} \frac{R_b}{\mu} \text{ grad } T \qquad \text{(Eq 20)}$$

In view of the lack of experimental data, we estimate $\mu \simeq (1 - 10) \times 10^{-3}$ kg/ms. The temperature gradient implied by numerical modeling (see Fig. 2) is on the order of 100 K/R_0. Then, a bubble of radius $R_b = R_0/10$ moves with velocity $v \simeq (0.1 - 1)$ m/s, a value higher than the velocity of the solid/liquid boundary motion during the process in question (again, see Fig. 2).

According to Eq 17, the final cavity radius is $R_c \simeq 0.67\, R_0$, a value precisely confirmed in Fig. 2.

4. Concluding Remarks

It has been shown that the formation of a cavity in a solidifying drop starts from vapor bubble. The reason is the cavitation phenomenon in response to a pressure decrease that occurs due to the lack of material under the growing solid shell. (The possible reabsorption of a gas has not been considered.) The balance of pressures acting in the melted material and in the bubble (Eq 6) implies the minimum bubble radius (Eq 8), which does not depend on the mass densities—ρ_m, ρ_s—of the melted and solid phases.

The following physical picture concerns the stability of solution of Eq 6 with respect to the unknown R_b. If the solution $R_{b1} < R_b^{min}$ occurs, the value of R_{b1} decreases with an increase of solid shell thickness ΔR_s. Simultaneously, the pressure in the liquid phase further decreases. Consequently, this liquid is unstable with respect to nucleating a bubble with the larger radius $R_{b2} > R_b^{min}$. If a new bubble arises, the first bubble collapses under the action of the surface tension. Then, the radius R_{b2} increases with the growing shell thickness and the process is stable. This is also the reason why *only one* cavity can occur.

The necessary (Eq 11) and sufficient (Eq 12) conditions of a stable bubble existence give the minimum thickness of the solid shell at the bubble formation. This shell is very thin, implying that the bubble is born at the very early stage of the droplet solidification.

The motion driven by the surface tension inhomogeneity in a temperature gradient is thermophoretic effect. It can be significant when the bubble arises outside the temperature maximum.

The radii of the resulting cavities ($R_c \simeq 2R_0/3$) calculated from our theory are somewhat larger than those found in experiments (Ref 2). The reason is that the atmospheric pressure can diminish the solidifying particle radius R_0. This effect should be estimated after the values of necessary material constants are known, namely, the creep behavior of solid alumina at high temperatures.

On the other hand, the experimentally found cavity volume V_{ce} implies that the value of the particle radius decreases by ΔR_{atm}, which occurs due to the atmospheric pressure. Comparing V_{ce} with the theoretical value V_c in Eq 16 and neglecting the dilatation proportional to α_v yields the following simple relation:

$$\frac{\Delta R_{atm}}{R_0} \simeq \frac{V_c - V_{ce}}{3V_c}\left(1 - \frac{\rho_m}{\rho_s}\right)$$

For alumina particles, this value is approximately 0.1 or less. Craters (open surface voids) found on some spheroidized particles result from asymmetry of the solid shell formation and the simultaneous action of the atmospheric pressure.

Acknowledgment

The authors are indebted to Professor P. Chráska for permanent support during this work.

References

1. O.V. Romanov, Ed , *Gas-thermic Processing of Ceramic Oxides*, Nauka i Tekhnika, Minsk, 1988, p 93 (in Russian)
2. J. Dubsky, B. Kolman, and V. Brozek, Plasma Technology Preparing of Metal and Ceramic Powders, *Methods of Preparing and Characterization of Powder Materials*, University of Chemical Technology, Pardubice, Czech Republic, 1993, p 13 (in Czech); K. Neufuss, Institute of Plasma Physics, Academy of Sciences of Czech Republic, Prague, private communication, 1995
3. I.K. Kikoin, Ed., *Tables of Physical Values*, Atomizdat, Moscow, 1976, p 192, 203, 250 (in Russian)
4. L.D. Landau and E.M. Lifshits, *Theoretical Physics*, Vol VI, *Hydrodynamics*, Nauka, Moscow, 1986, p 100 (in Russian)
5. P. Kotalík, On a Numerical Approach to Stefan Problem, *J. Phys. III France*, Vol 3 (No. 11), 1993, p 2113-2120